arXiv:cond-mat/0105605v1 [cond-mat.supr-con] 31 May 2001

Proximity Effect and Multiple Andreev Reflections in Chaotic Josephson junctions

P. Samuelsson, G. Johansson, Å. Ingerman, V.S. Shumeiko, and G. Wendin
Department of Microelectronics and Nanoscience, Chalmers University of Technology and Göteborg University, S-41296 Göteborg, Sweden
(February 1, 2008)

We study the dc-current transport in a voltage biased superconductor-chaotic dot-superconductor junction with an induced proximity effect(PE) in the dot. It is found that for a Thouless energy E_{Th} of the dot smaller than the superconducting energy gap Δ, the PE is manifested as peaks in the differential conductance at voltages of order E_{Th} away from the even subharmonic gap structures $eV \approx 2(\Delta \pm E_{Th})/2n$. These peaks are insensitive to temperatures $kT \ll \Delta$ but are suppressed by a weak magnetic field. The current for suppressed PE is independent of E_{Th} and magnetic field and is shown to be given by the Octavio-Tinkham-Blonder-Klapwijk theory.[1]

Over the last decades, there has been a large interest in various aspects of the proximity effect (PE) in mesoscopic normal conductor-superconductor (NS) systems. The PE can on a microscopic level be viewed as correlations on the scale of the Thouless energy E_{Th} between electrons and holes in the normal conductor, induced via Andreev reflections at the NS-interface. Well known manifestations of the PE are the bias conductance anomaly[2] in diffusive NS-junctions and the induced gap in the spectrum of diffusive[3] or chaotic[4] SNS- and NS-junctions.

There is however no complete theory of the PE in voltage biased SNS-junctions. The reason is that electrons and holes in the normal conductor undergo multiple Andreev reflections[1,5] (MAR), giving rise to complicated correlation effects and strong nonequilibrium in the normal part of the junction.[6] The fingerprint of MAR transport is subharmonic gap structures (SGS) in the current-voltage characteristics at $eV = 2\Delta/n$.

So far only some limiting cases have been considered. In short junctions, where E_{Th} is much larger than the superconducting energy gap Δ, a coherent MAR-theory[7] has been developed which fully incorporates the PE. The theory describes to large accuracy experiments in atomic size point contacts[8] and has also been applied to short diffusive junctions[9] and disordered tunnel barriers.[10] For junctions in the short limit, the PE modifies the shape but not the position of the SGS, as well as gives rise to ac-Josephson effect. Other cases studied are long, $E_{Th} \ll \Delta$, diffusive SNS-junction with no proximity coupling between the superconductors[11] and SNS-junctions consisting of two weakly coupled proximity NS-junctions in equilibrium.[12]

Taken together, present theories do not give an answer to the general question of the role of the PE in SNS-junctions where the Thouless energy is comparable to the superconducting energy gap, $E_{Th} \sim \Delta$. Moreover, recent experiments on SNS-junctions in this regime[13] show qualitatively new features: splitting of the SGS conductance peaks at even subharmonics $eV = \Delta$ and $\Delta/2$.

In this Letter we study current transport in a superconductor-chaotic dot-superconductor (S-dot-S) junction. By employing the scattering theory of MAR[14] and using random matrix theory[15] to describe the statistical properties of the energy- and magnetic field dependent scattering matrix of the dot, we are able to calculate the dc-current for arbitrary ratio between E_{Th} and Δ as well as for arbitrary strength of the PE due to variation of the magnetic field in the dot.[4]

The main result of the paper is the explanation of the splitting of the even SGS conductance peaks, i.e the additional peaks at $eV \approx 2(\Delta \pm E_{Th})/2n$, in terms of an induced PE in the dot. The PE conductance peaks are suppressed by a weak magnetic field but are insensitive to temperatures $kT \ll \Delta$.

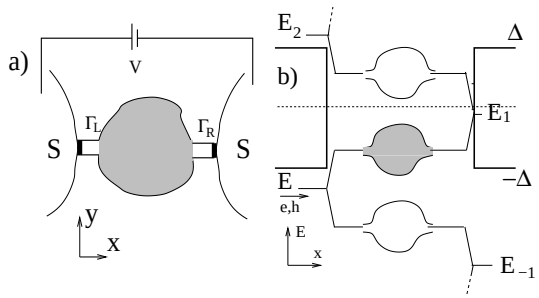

FIG. 1. a) Schematic picture of the junction. The shaded region is the chaotic dot and the black bars denote tunnel barriers with transparency Γ_L and Γ_R. b) A MAR-trajectory in energy-position space for quasiparticles injected at energy E from left. Filled (empty) chaotic dots denote electrons (holes) scattering. Scattering processes in which quasiparticles are Andreev reflected at energies E_{Th} away from the Fermi energy have an enhanced amplitude, giving rise to additional peaks in the conductance at $eV \approx 2(\Delta \pm E_{Th})/2n$.

The junction is shown schematically in Fig.1: A two-dimensional quantum dot is coupled to two superconducting electrodes via quantum point contacts supporting N transverse modes each. The contacts contain tunnel barriers with mode-independent transmission probabilities $\Gamma_L, \Gamma_R \gg 1/N$. It is assumed that the quasiparticle dwell time in the dot, $\hbar/E_{Th}$, is much smaller than the inelastic scattering time; here $E_{Th} = N(\Gamma_L + \Gamma_R)\delta/(2\pi)$ and δ is mean level spacing of the dot. In this case the transport through the junction can be characterized by the Andreev reflection amplitudes at the normal lead-insulator-superconductor (NIS) interfaces and the scat-

tering matrix of the dot. We consider the case where the classical motion in the dot is chaotic on time scales longer than the ergodic time $\tau_{erg} \sim L/v_F$ ($l \gg L$) or $L^2/(lv_F)$ ($l \ll L$), where L and l are the linear dimension and the mean free path of the dot. The ergodic time is assumed to be smaller than the quasiparticle dwell time and the inverse superconducting gap, $\tau_{erg} \ll \hbar/E_{Th}, \hbar/\Delta$. In this case random matrix theory[15] can be used to describe the scattering properties of the dot.

The scattering matrix S can be written in terms of the Hamiltonian H (dimension M) of the closed dot as

$$S = \begin{pmatrix} r & t' \\ t & r' \end{pmatrix} = 1 - 2\pi i W^\dagger (E - H + i\pi W W^\dagger)^{-1} W, \tag{1}$$

where r, t, r' and t' are the $N \times N$ reflection and transmission matrices and W describes the coupling of the dot to the leads, with $W_{nm} = \delta_{nm}(M\delta)^{1/2}/\pi$. The Hamiltonian H is described by a random Hermitian matrix $H = H_0 + i\gamma H_1$, where H_0 and H_1 are real symmetric and anti-symmetric matrices respectively, independently distributed with the same Gaussian distribution, $P(H_{0(1)}) \propto \exp[-\pi^2(1+\gamma^2)\mathrm{tr}(H_{0(1)}H^T_{0(1)})/(4M\delta^2)]$. The parameter γ is related to the magnetic flux in the dot as $\Phi \simeq \gamma\Phi_0(M\delta\tau_{erg}/\hbar)^{1/2}$,where $\Phi_0 = h/e$ is the flux quantum. A magnetic flux $\Phi_c \simeq \Phi_0(\tau_{erg}E_{Th}/\hbar)^{1/2}$ effectively breaks time reversal symmetry in the dot.

The current is calculated within a scattering approach for the Bogoliubov-de Gennes equations[14] and is expressed in terms of the scattering state wavefunctions Ψ_σ, as $I = (e/h)\int dy \sum_\sigma \mathrm{Im}(\Psi^\dagger_\sigma[d\Psi_\sigma/dx])f_0$, where $\sigma = \{e/h, E, L/R, j\}$ labels the scattering state (electron/hole like quasiparticle injected at energy E from the left/right superconducting reservoir, in transverse mode j) and f_0 is the equilibrium Fermi distribution of the reservoirs. The energies are measured relative to the Fermi energy in the superconductors and the magnetic field in the contacts is assumed to be zero.

The acceleration of the injected quasiparticles due to the applied voltage V gives a scattering state wavefunction which is a superposition of electron and hole states at different energies[14] $E_n = E + 2neV$. For quasiparticles incident from the left superconductor, the wavefunction on the normal side of the left NIS-interface has the form

$$\Psi_L = \sum_{m=1}^{N} \Phi_m(y) \sum_n e^{-iE_{2n}t/\hbar} \times \begin{bmatrix} (c^{e,+}_{m,2n} e^{ik^e_{m,2n}x} + c^{e,-}_{m,2n} e^{-ik^e_{m,2n}x})/(k^e_{m,2n})^{1/2} \\ (c^{h,+}_{m,2n} e^{ik^h_{m,2n}x} + c^{h,-}_{m,2n} e^{-ik^h_{m,2n}x})/(k^h_{m,2n})^{1/2} \end{bmatrix} \tag{2}$$

where m is transverse mode index. At the right interface the electron/hole energies are shifted by $\pm eV$ and the wave function Ψ_R is given by multiplying Ψ_L by $\exp(-i\sigma_z eVt/\hbar)$ and substituting $2n \to 2n+1$ (σ_z is the Pauli matrix in electron-hole space). The wave vector $k^{e(h)}_{m,n} = [(2m/\hbar^2)(E_F - \epsilon_m \pm E_n)]^{1/2}$, where ϵ_m is the transverse mode energy and $+/-$ corresponds to electrons/holes. The vector potential enters only the transverse wavefunctions Φ_m, normalized for each mode to carry the same current. The scattering at the dot connects the electron and hole wavefunction coefficients as

$$\begin{pmatrix} \hat{c}^{e,-}_n \\ \hat{c}^{e,+}_{n+1} \end{pmatrix} = S^+_n \begin{pmatrix} \hat{c}^{e,+}_n \\ \hat{c}^{e,-}_{n+1} \end{pmatrix}, \begin{pmatrix} \hat{c}^{h,+}_n \\ \hat{c}^{h,-}_{n-1} \end{pmatrix} = S^-_n \begin{pmatrix} \hat{c}^{h,-}_n \\ \hat{c}^{h,+}_{n-1} \end{pmatrix}, \tag{3}$$

where we have introduced the vector notation $\hat{c}^{e,+}_n = [c^{e,+}_{1,n}, ..., c^{e,+}_{N,n}]$ and $S^+_n = S(E_n)$ and $S^-_n = S^*(-E_n)$. At the left NIS-interface, the scattering is described by Andreev and normal reflection and transmission amplitudes for electrons (e) and holes (h), $a^{e/h}_n = a^{e/h}(E_n)$ and similarly $b^{e/h}_n$, $c^{e/h}_n$ and $d^{e/h}_n$, given in Ref. 16. This gives the connection between wavefunction coefficients as

$$\begin{pmatrix} \hat{c}^{e,-}_n \\ \hat{c}^{h,+}_n \end{pmatrix} = \begin{pmatrix} b^e_n & a^h_n \\ a^e_n & b^h_n \end{pmatrix} \begin{pmatrix} \hat{c}^{e,+}_n \\ \hat{c}^{h,-}_n \end{pmatrix} + \delta_{n0}\delta_{mj} \begin{pmatrix} c^e_n \\ d^e_n \end{pmatrix}, \tag{4}$$

where the source term ($\propto \delta_{n0}\delta_{mj}$) describes electron quasiparticle injection. The coefficients at the right NIS-interface are connected in a similar way. The other scattering states are constructed analogously.

In the short dwell time regime, $E_{Th} \gg \Delta$, the scattering matrix is independent of energy on the scale of Δ, and the current can be written[9,10] as a sum of the single mode currents[7], with different transmission eigenvalues D_m (eigenvalues of the matrix product $tt^\dagger$). The ensemble averaged current $\langle I \rangle$ is then found via an integration over transmission eigenvalues with the distribution[17] $\rho(D) = N/\pi[\Gamma(2-\Gamma)]/([\Gamma^2 + 4D(1-\Gamma)]\sqrt{D(1-D)})$. The current voltage characteristics in Fig. 2a show SGS at $eV = 2\Delta/n$ and an excess current[18] for all Γ [the normal state conductance $G_N = (2e^2/h)N\Gamma_L\Gamma_R/(\Gamma_L+\Gamma_R)$].

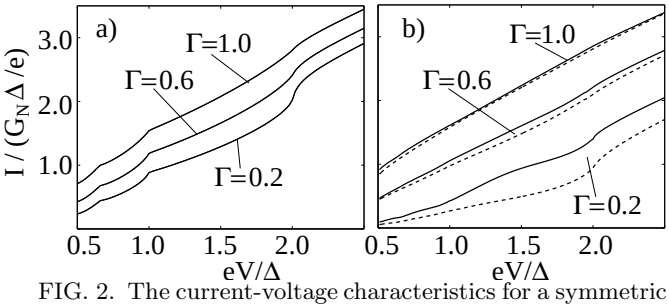

FIG. 2. The current-voltage characteristics for a symmetric junction $\Gamma = \Gamma_L = \Gamma_R$ with a temperature $kT \ll \Delta$. a) In the short dwell time regime, $E_{Th} \gg \Delta$, the current show SGS at $eV = 2\Delta/n$. b) In the intermediate dwell time regime, $E_{Th} = 0.4\Delta$, the current is shown for $\Phi = 0$ (solid) and $\Phi \gg \Phi_c$ (dashed) and $N = 10$. The SGS is less pronounced and the current for low transparencies is smaller compared to the short dwell time regime.

For a longer quasiparticle dwell time, $E_{Th} \lesssim \Delta$, the ensemble averaged current is calculated numerically by generating a large number of Hamiltonians.[19] The current voltage characteristics is shown in Fig. 2b for

$E_{Th} = 0.4\Delta$. Compared to the short dwell time regime in Fig 2a, the SGS is less pronounced and the current for low barrier transparencies is reduced for $\Phi = 0$ and even further for $\Phi \gg \Phi_c$.

The current voltage characteristics can be studied in detail by considering the conductance, dI/dV, shown in Fig. 3 (parameters chosen to clearly display PE-features). The conductance with suppressed PE, $\Phi \gg \Phi_c$, shows SGS at $eV = 2\Delta/n$. The PE is manifested as an enhancement of the SGS at $eV = \Delta$ but also as additional peaks[20] in the conductance on both sides of $eV = \Delta$. It is found by varying E_{Th} that the positions of the additional peaks are given by $eV \approx \Delta \pm E_{Th}$. Moreover, the position and magnitude of the peaks are found to be insensitive to temperatures $kT \ll \Delta$.

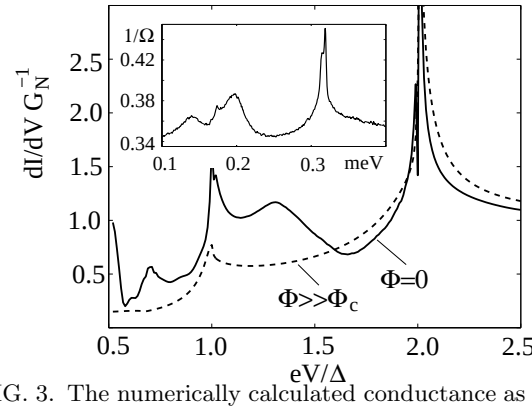

FIG. 3. The numerically calculated conductance as a function of voltage for $\Gamma_L = 0.1, \Gamma_R = 0.3$, $E_{Th} = 0.4\Delta$, $kT \ll \Delta$ and $N = 15$. Inset: The differential conductance as a function of voltage for the diffusive SNS-junction, $L = 0.29\mu m$ and $\Delta = 0.17meV$ at $kT = 240mK$, studied experimentally by Kutchinsky et al.[13] The theoretical and experimental curves show the same qualitative features with conductance peaks at $eV = 2\Delta, \Delta$ and $\Delta \pm E_{Th}$.

These features of the conductance have recently been observed[13,21] in experiments with diffusive SNS-junctions of intermediate length, $E_{Th} \lesssim \Delta$ (shown as inset in Fig. 3). The experimental curves show conductance peaks at $eV \approx 2\Delta, \Delta, \Delta \pm E_{Th}$ and $eV \approx (\Delta \pm E_{Th})/2$, with position and amplitude insensitive to temperatures $kT \ll \Delta$. In a corresponding interferometer setup[13] the peaks at $eV \approx \Delta \pm E_{Th}$ are demonstrated to result from induced PE (the peaks at $eV \approx (\Delta \pm E_{Th})/2$ could not be resolved). The amplitude of all SGS peaks is successively reduced for increasing junction length, and the peaks at $eV \approx \Delta \pm E_{Th}$ are washed out in long junctions, $E_{Th} \ll \Delta$. Although the system studied experimentally is different from a S-dot-S junction, the two type of junctions can be expected to show qualitatively similar behavior, in the same way as for an NS and a N-dot-S junction (see Ref. 22).

A qualitative understanding of the origin of the PE conductance peaks can be obtained by first considering the peak at $eV \approx \Delta + E_{Th}$. It is built up by quasiparticles which are Andreev reflected once at energies of order of E_{Th} away from the Fermi energy (see Fig. 1b). These scattering processes have enhanced amplitude due to the PE and are similar to the ones giving rise to the finite bias conductance anomaly in NS-junctions.[2] The conductance peak is insensitive to temperatures $kT \ll \Delta$, since the distribution of injected quasiparticles from the superconductors is unaffected by temperatures well below the superconducting gap, in contrast to the NS-conductance anomaly, which is suppressed for $kT \gg E_{Th}$.

The conductance peak at $eV \approx \Delta - E_{Th}$ results from scattering processes which include two Andreev reflections, with one of the reflections at an energy of order E_{Th} away from the Fermi energy. These process, in the same way, have an enhanced amplitudes due to the PE. Since the processes with one and two Andreev reflections are different, the shape and amplitude of the conductance peaks at $eV \approx \Delta \pm E_{Th}$ are in general different. Following the same line of reasoning, we predict that the conductance (for E_{Th} smaller than the distance between subsequent subgap harmonics) will show peaks at all $eV \approx 2(\Delta \pm E_{Th})/(2n)$.

It follows from the quantum mechanical current expression that the ensemble averaged dc-current can be written as $\langle I \rangle = N(e/h) \sum_{\sigma,n} (f^{e,+}_{n,\sigma} - f^{e,-}_{n,\sigma} + f^{h,+}_{n,\sigma} - f^{h,-}_{n,\sigma})$, where $f^{e/h,\pm}_n = \langle \mathrm{tr}[(\hat{c}^{e/h,\pm}_n)^\dagger \hat{c}^{e/h,\pm}_n] \rangle f_0/N$ (suppressing index σ) are correlation functions of the wavefunction coefficients and the trace is taken over the transverse modes. The functions $f^{e/h,\pm}_n$ can be interpreted as ensemble averaged distribution functions at energy E_n for electron/hole quasiparticles with positive/negative sign of the wavenumber, summed over transverse modes. For broken time reversal symmetry in the dot, $\Phi \gg \Phi_c$, it is possible to formulate matching equations for the distribution functions $f^{e/h,\pm}_n$ directly, in the following way:

We first note that for quasiparticles propagating in energy-position space along the MAR-ladder (see Fig. 1b), the scattering matrices of the dot at different energies are effectively uncorrelated to leading order in $N\Gamma_L, N\Gamma_R$, (i.e. neglecting quantum corrections). This result is an extension of what is found for an N-dot-S junction,[17] by employing the same diagrammatic technique for integration over the unitary group.

The statistical independence of the scattering matrices leads to three rules for wavefunction coefficient correlations and averages: i) coefficients with different energy indices n are uncorrelated since they are connected via at least one traversal through the dot. (This also means that there is no ac-Josephson current.) ii) coefficients for quasiparticles incoming towards the NIS-interface are uncorrelated, because incoming quasiparticles have scattered at dots at different energies before approaching the NIS-interface. iii) the average of any coefficient itself is zero. With these rules for the correlations between different wavefunction coefficients, we can, directly from the matching Eqs. (3) and (4), derive matching equations for the functions $f^{e/h,\pm}_n$. For the scattering across the dot,

e.g. for left injected electrons, we get from Eq. (3)

$$f_n^{e,-} = \langle \mathrm{tr}\left[(r\hat{c}_n^{e,+} + t'\hat{c}_{n+1}^{e,-}) \times c.c.\right]\rangle = 1/2[f_n^{e,+} + f_{n+1}^{e,-}]$$
$$f_{n+1}^{e,+} = 1/2[f_{n+1}^{e,-} + f_n^{e,+}]. \quad (5)$$

In this derivation we used that the averaging rules gives $\langle \mathrm{tr}[(\hat{c}_{n+1}^{e,-})^\dagger t'^\dagger t' \hat{c}_{n+1}^{e,-}]\rangle = \langle \mathrm{tr}(t'^\dagger t')\rangle \langle \mathrm{tr}[(\hat{c}_n^{e,-})^\dagger \hat{c}_n^{e,-}]\rangle/N$ and similarly for the other terms. Also, the averages $\langle \mathrm{tr}(t'^\dagger t')\rangle = \langle \mathrm{tr}(r^\dagger r)\rangle = N/2$. From Eq. (4), the matching equations at the left NIS-interface become

$$\begin{aligned} f_n^{e,-} &= \langle \mathrm{tr}\left[(b_n^e \hat{c}_n^{e,+} + a_n^h \hat{c}_n^{h,-} + c_n^e \delta_{n0}) \times c.c.\right]\rangle \\ &= B_n f_n^{e,-} + A_n f_n^{h,+} + C_n f_0 \delta_{n0}, \\ f_n^{h,+} &= A_n f_n^{e,+} + B_n f_n^{h,-} + D_n f_0 \delta_{n0}, \end{aligned} \quad (6)$$

where the scattering probabilities[16] $A_n = |a_n^{e/h}|^2$ and similarly B_n, C_n and D_n, have been introduced. The total distribution function for right (left) going electrons on the left side at energy E', $f^L_{\rightarrow(\leftarrow)}(E')$ is found by summing up the distribution functions for right(left) going electrons from all scattering states σ. From Eq. (6), it follows that the total distribution functions at the left NIS-interface are related as

$$\begin{aligned} f^L_{\rightarrow}(E') = A(E')[1 - f^L_{\leftarrow}(-E')] + B(E') f^L_{\leftarrow}(E') \\ + T(E') f_0(E'), \end{aligned} \quad (7)$$

where $T(E') = C(E') + D(E') = 1 - A(E') - B(E')$. In this derivation we also used the symmetry for the total distribution functions $f^e(E') = 1 - f^h(-E')$, which can be derived directly from Eqs. (5) and (6). The relations between the total distribution functions at the right interface and across the dot follow in the same way. The resulting set of equations corresponds exactly to the matching equations for distribution functions in Ref. 1 (OTBK), with the important exception that the scattering by the dot itself couples the left- and right moving distributions of electrons in the normal part of the junction (i.e. a SINI'NIS junction with transparency 1/2 of I'). The current is given by $\langle I\rangle = 1/(eR_0)\int dE'[f_{\rightarrow}(E') - f_{\leftarrow}(E')]$, with $R_0 = h/(2e^2N)$. This shows that the OTBK-approach can be rigorously justified for a S-dot-S junction with broken time reversal symmetry in the dot.

We notice that the presented derivation is also applicable to a long diffusive wire ($l \ll L$) SNS-junction with time reversal symmetry broken in the wire. The only difference is that the middle barrier (I') now has a transmission probability l/L.

In conclusion, we have studied the dc-current transport in a voltage biased S-dot-S junction with an induced PE in the dot. It is found that the PE is manifested as peaks in the conductance at voltages $eV \approx 2(\Delta \pm E_{Th})/2n$. These peaks are insensitive to temperatures $kT \ll \Delta$ but are suppressed by a weak magnetic field. The current for suppressed PE is independent of E_{Th} and magnetic field and is shown to be given by the OTBK-theory.

We thank J. Kutchinsky for making the experimental data presented in the paper available and we acknowledge helpful discussions with E. Bezuglyi, J. Kutchinsky, J. Bindslev-Hansen, J. Lantz and H. Schomerus. This work was supported by TFR, NEDO and NUTEK.

[1] M. Octavio et al., Phys. Rev. B. **27**, 6739 (1983)
[2] A. Kastalsky et al., Phys. Rev. Lett. **67**, 3026 (1991).
[3] A.A. Golubov and M. Yu. Kuprianov, Sov. Phys. JETP **69**, 805 (1989); W. Belzig, C. Bruder, and G. Schön, Phys. Rev. B. **54**, 9443 (1996); S. Gueron et al., Phys. Rev. Lett. **77** 3025 (1996).
[4] J. Melsen et al., Europhys. Lett **35**, 7 (1996).
[5] T.M. Klapwijk, G.E.Blonder, and M. Tinkham, Physica B+C **109-110**, 1657 (1982).
[6] E.V. Bezuglyi et al., Phys. Rev. Lett. **83** 2050 (1999), F. Pierre, *ibid.* **86**, 1078 (2001).
[7] G.B. Arnold, J. Low Temp. Phys. **68**, 1 (1987), E.N. Bratus', V.S. Shumeiko, and G.Wendin, Phys. Rev. Lett. **74**, 2110 (1995); D. Averin, and A. Bardas, **ibid 75**, 1831 (1995); J.C. Cuevas, A. Martin-Rodero, and A.L. Yeyati, Phys. Rev. B. **54**, 7366 (1996).
[8] N. van der Post et al., Phys. Rev. Lett. **73**, 2611 (1994); E. Scheer et al., *ibid.* **78**, 3535 (1997).
[9] A. Bardas and D. Averin, Phys. Rev. B. **56**, R8518 (1997).
[10] Y. Naveh et al., Phys. Rev. Lett. **85**, 5404 (2000).
[11] E.V. Bezuglyi et al., Phys. Rev. B **62**, 14439 (2000).
[12] B.A. Aminov, A.A. Golubov, and M.Yu. Kupriyanov, Phys. Rev. B. **53**, 365 (1996), A.V. Zaitsev and D.V. Averin, Phys. Rev. Lett. **80**, 3602 (1998), E. Scheer et al. ibid **86**, 284 (2001).
[13] J. Kutchinsky et al., Phys. Rev. B **56**, R2932 (1997); R. Taboryski et al., Superlatt. and Microstr. **25**, 829, (1999).
[14] See e.g. G. Johansson et al. Superlatt. and Microstr. **25**, 906, (1999) and references therein.
[15] C.W.J. Beenakker, Rev. Mod. Phys, **69**, 731 (1997); Y. Alhassid, *ibid* **72**, 895 (2000).
[16] G.E. Blonder, M. Tinkham and T. M Klapwijk, Phys. Rev. B. **25**, 4515 (1982).
[17] P.W. Brouwer and C.W.J. Beenakker, J. Math. Phys. (N.Y.) **37**, 4904 (1996).
[18] The excess current is ranging from $(G_N e/\Delta)[16/3+\pi(9/2-4\sqrt{2})]$ for $\Gamma = 1$ to $(G_N e/\Delta)[\pi/4(7-4\sqrt{2})]$ for $\Gamma \ll 1$. In the limit $\Gamma \ll 1$ the distribution $\rho(D)$ is the same as for a dirty tunnel barrier and the result coincides with Ref. 10.
[19] In all numerical curves shown, $M = 20N$ and 1000 Hamiltonians have been generated for each curve.
[20] For large interface transparency $\Gamma_L, \Gamma_R \sim 1$, the conductance peaks turn into dips.
[21] Additional features in the SGS has also been observed in A. Chrestin, T Matsuyama and U. Merkt, Phys. Rev. B **55**, 8457 (1997) and T. Schäpers et al, Superlatt. and Microstr. **25**, 851, (1999).
[22] A.A. Clerk, P.W. Brouwer, and V. Ambegaokar, Phys. Rev. B **62**, 10226 (2000).